Biol. Cybern. 88, 210–218 (2003)
DOI 10.1007/s00422-002-0377-3


Biological Cybernetics

# Deriving physical connectivity from neuronal morphology

**Nir Kalisman**[1], **Gilad Silberberg**[1,2], **Henry Markram**[2]

[1] Department of Neurobiology, Weizmann Institute of Science, Rehovot 76100, Israel
[2] Brain and Mind Institute, EPFL, Lausanne 1015, Switzerland

Received: 11 February 2002 / Accepted: 5 November 2002 / Published online: 20 February 2003

**Abstract.** A model is presented that allows prediction of the probability for the formation of appositions between the axons and dendrites of any two neurons based only on their morphological statistics and relative separation. Statistics of axonal and dendritic morphologies of single neurons are obtained from 3D reconstructions of biocytin-filled cells, and a statistical representation of the same cell type is obtained by averaging across neurons according to the model. A simple mathematical formulation is applied to the axonal and dendritic statistical representations to yield the probability for close appositions. The model is validated by a mathematical proof and by comparison of predicted appositions made by layer 5 pyramidal neurons in the rat somatosensory cortex with real anatomical data. The model could be useful for studying microcircuit connectivity and for designing artificial neural networks.

## 1 Introduction

The cerebral cortex is a vast ensemble of highly branched neurons intermingled in a complex way. The growth of an axonal arborization of one neuron into the dendritic span of a second allows the two neurons to contact each other through synapses, which enables activity to flow between neurons. Isolating the geometrical factors that determine the probability and location of synapses that one neuron will form with another is, therefore, important for understanding how neural microcircuits, which underlie brain function, are formed. A necessary but insufficient condition for functional synapses is the availability of a physical contact between the membranes of the presynaptic axon and the postsynaptic dendrite. This nonsufficiency is revealed by electron microscope images (White 1989) showing that contacts between axons and dendrites exist without synaptic specialization. Nevertheless, physical proximity of pre- and postsynaptic elements is important for understanding functional connectivity because it provides the upper limit for the possible number of synaptic contacts. Such a limit could be useful in estimating the potential for synaptic connectivity and provide insight into the principles of microcircuit formation.

The two key factors that determine physical connectivity between a pair of neurons are their respective morphologies and relative positions. Physical connectivity may also be influenced by nongeometrical factors such as specific chemical attractors or repellents. The influence of these nongeometrical factors in the cortex is poorly understood and will not be considered in this study. Restricting the study to geometrical factors requires a model that can predict how often any axonal arbor will form a close apposition with a dendritic arbor based only on their morphologies and separation. The first attempt to derive such a model was proposed by Uttley (1956) and later extended by Liley and Wright (1994). In their model, the axonal and dendritic trees were reduced to a collection of intermingled straight segments. The probability of forming close appositions between axonal and dendritic segments was derived from their respective densities in space. Braitenberg and Schüz (1998) adopted a simpler approach. They took advantage of the observation that collaterals of pyramidal axons tend to stretch for relatively long distances in a remarkably straight line. An axonal collateral might be modeled as "shooting" through the dendritic arbor of the postsynaptic neuron. Under such conditions, the dendritic arbor was projected onto a plane perpendicular to the direction of the axonal collateral, and the chance for an apposition to be made was proportional to the dendritic density on the projection plane. Hellwig (2000) proposed a different way of estimating connectivity from morphology. According to this method, 3D reconstructions of two neurons were superimposed and shifted relative to each other. A physical contact was indicated if axonal and dendritic elements shared the same 1-μm voxel. By averaging over many relative positions of the two neurons

*Correspondence to*: H. Markram
(e-mail: Henry.Markram@epfl.ch
Tel.: +41-21-6939537, Fax: +41-21-6935350)

and over many reconstructions of the same type of neuron, statistics for the physical connectivity for that type of neuron was derived.

This paper provides a model for the derivation of physical connectivity from morphology, which is closer to the model of Liley and Wright (1994). We discard, however, two assumptions that were fundamental in their model and are not generally correct in neurons. Their model assumed that axonal and dendritic arbors are spherically symmetrical. It also ignored branching directionality; only absolute branching density was used in the calculations. The method presented here does not rely on these assumptions, rendering it much more applicable to real neurons. In this model, statistical representations obtained from 3D reconstructions of the same cell type are "averaged" in a novel way to form two spatial-density maps that capture the relevant morphological features of the cell type. These two maps are referred to as the axonal and dendritic "templates." It is argued that these two templates provide all the information required to estimate the average number of physical contacts formed by a pair of neurons of that type, given any relative separation of their cell bodies. Additional characteristics of connections are also extracted such as the likely locations of contacts and the average axonal and dendritic lengths from the cell body to contact points. The model is tested on real morphological data obtained from reconstructions of layer 5 pyramidal neurons of the rat somatosensory cortex.

## 2 Materials and methods

### *2.1 Intracellular labeling with biocytin and histology*

Neocortical slices (sagittal, 300 μm thick) were obtained from Wistar rats (14–16 d old). Slices were incubated for 30 min at 35 °C and then at room temperature (20∼22 °C) until transferred to the recording chamber (32∼34 °C). Pyramidal cells in layer 5 of the somatosensory area were selected for recording according to the morphology of their somata and proximal dendrites. The slice was visualized by IR-DIC optics using a Zeiss Axioscope and Hamamatsu CCD camera. The bathing solution consisted of (in mM): NaCl 125, $NaHCO_3$ 25, glucose 25, $CaCl_2$ 2, $NaH_2PO_4$ 1.25, $MgCl_2$ 1. Whole-cell recordings were made using patch pipettes (5–10 MΩ), containing (in mM) K-gluconate 110, KCl 10, HEPES 10, phosphocreatine(Na) 10, MgATP 4, NaGTP 0.3, and biocytin 4 mg/ml. Somata of recorded cells were located at least 40 m (average: 70 M) below the slice surface to enable reliable morphological reconstruction. Voltage recordings were obtained using axopatch 200/B amplifiers (Axon Instruments). Subsequent recording slices were fixed with 0.1 M phosphate-buffered solution containing 2% paraformaldehyde and 2% glutaraldehyde, for a period of 24–48 h. Slices were then washed with phosphate-buffer and stained with standard biocytin staining kit based on avidin-conjugated horseradish peroxidase (ABC-Elite Vector Labs). Immediately following staining, slices were flattened on glass slide in ImmuGlo mounting medium (Immco Diagnostics, NY) and covered with cover slips.

### *2.2 3D reconstructions*

Only stained cells that showed high staining contrast were chosen for reconstruction. It was common for cells to have good staining contrast in the dendrites while only faint staining of the axon. In such cases only the dendritic tree was reconstructed. 3D reconstruction was done with the Neurolucida system (MicroBrightField, Colchester, VT) using an Olympus X60 water-immersed objective. Tissue shrinkage in the direction perpendicular to the plane of sectioning was estimated to be 11% by comparing the average slice thickness after mounting, 265 μm, to the original thickness setting of the vibratome, 300 μm. The shrinkage factor parallel to the sectioning plane was not measured and was considered to be the same. The reconstruction data were therefore scaled by a factor of 1.13 in all three axes. The depth of the cell bodies below the slice surface was different in every reconstruction. In order to average the reconstructions, such nonuniformity should be eliminated. We therefore artificially deleted every structure that was higher than 30 μm above the cell body toward the slice surface.

### *2.3 Averaging the reconstructions into templates*

The creation of the axonal and dendritic templates requires the averaging of many reconstructions together. For their proper alignment, a general coordinate system is introduced. The origin of the system is defined as the point where the main axonal trunk leaves the cell body. In pyramidal neurons this point is clear and well defined. The $y$-axis is defined as the direction parallel to the apical dendrite. The $x$-axis is defined as orthogonal to the $y$-axis and parallel to the plane of sectioning of the slice. Since parasagittal slices were used, the $x$-axis is parallel to the rostral-caudal direction. The $z$-axis is orthogonal to the $x, y$-axes, pointing to the depth of the slice. By using these general coordinates, all the reconstructions could be translated and rotated to enable a coherent alignment with each other.

For the creation of the axonal template the branching neuron is viewed as the source of a flux of axonal segments filling space in various directions. The axonal template, $F_A(\boldsymbol{r}, \Omega)$, is a function of two variables, position ($\boldsymbol{r}$) and direction ($\Omega$) in space. It is defined as the average number of axon collaterals around position $\boldsymbol{r}$, with direction $\Omega$ only, that pass through a 1-$\mu m^2$ area, situated perpendicular to the $\Omega$ direction. The units of the template are those of flux (segments/$\mu m^2$), and it gives a measure of the average flux of axon collaterals. For the purpose of calculating the connectivity, an axon segment stretching in direction $\Omega$ will form the same connections as a segment stretching in the $(-\Omega)$ direction. Therefore, while evaluating $F_A(\boldsymbol{r}, \Omega)$, segments with direction $(-\Omega)$ are added to the count of segments with direction $\Omega$. This invariance of positive-negative directionality is just one

example of why this is not real flux in the physical sense (i.e., it has no vectorial properties). The dendritic template, $F_D(\boldsymbol{r}, \Omega)$, is defined in the same way for the dendritic segments.

Creating templates for real neurons requires that both space and the directions in space be discrete. For the current study, space was divided into squared voxels with sides of 25 μm. Directions were indexed by considering only seven principal vectors: ($\{1,0,0\}$; $\{0,1,0\}$;$\{0,0,1\}$;$\{1,1,1\}$;$\{-1,1,1\}$;$\{1,-1,1\}$;$\{-1,-1,1\}$). The method of creating the templates is as follows. Each voxel is assigned seven counters corresponding to the seven principal directions. Each reconstruction is aligned to the general coordinates, and its branches are divided into 1-μm segments. For each segment the principal direction that is closest in absolute direction is found (absolute direction means either the principal vector itself or its exact opposite). The counter that corresponds to this principal direction in the voxel that contains that segment is incremented by 1. This process repeats for all the reconstructions that are to be averaged into the template. The template is then calculated by the normalization

$$F_{A,D}(\boldsymbol{r}, i) = \frac{C_{A,D}(\boldsymbol{r}, i)}{NV} \tag{1}$$

where $F_{A,D}(\boldsymbol{r}, i)$ is the value of the axonal/dendritic template for principal direction $i$ at voxel $\boldsymbol{r}$; $C_{A,D}(\boldsymbol{r}, i)$ is the counter for principal direction $i$ at voxel $\boldsymbol{r}$; $V$ is the voxel volume (in $\mu m^3$); and $N$ is the number of reconstructions averaged. Note that the volume, $V$, used in Eq. 1 should be the volume of the neuropil (cortical volume excluding cell bodies and blood vessels), that is 10–40% smaller than the total cortical volume depending on the brain area (Braitenberg and Schüz 1998). Results presented in this study do not include this neuropil correction since the fraction of the neuropil out of the total cortical volume was not measured.

Pyramidal neurons have cylindrical symmetry. The $y$-axis parallel to the apical dendrite is the axis of symmetry defined by the lamination of the cortex and several chemical gradients (Polleux et al. 2000). At the local environment around this axis, pyramidal neurons show relative uniform morphology (Anderson et al. 1999). Cylindrical symmetry is not a prerequisite of the model but is exploited specifically in this study for two purposes:

1. Reducing the number of reconstructions needed to get a reliable template. This is done by averaging together voxels that have the same $y$ value and the same distance from the $y$-axis, after proper rotation of their respective principal directions.
2. Even though the reconstruction of the neuron is incomplete due to the sectioning of the slice, the templates are completed by assigning missing voxels with the values of their symmetrical counterparts. In this way, connectivity can be evaluated for neurons in the intact cortex out of cut slices.

For the current study, the dendritic template of layer 5 pyramidal neurons was calculated by averaging dendrites from 14 neurons. Basal and apical dendrites were pooled together. The entire dendritic structure was averaged except the first 5 μm of each dendritic tree, since pyramidal neurons essentially do not form synapses on cell bodies and on the immediately proximal dendrites of other pyramidals (Peters and Jones 1984). The axonal template was calculated by averaging 11 reconstructed axons. The entire axonal structure was averaged except for the main trunk of the axon heading for the white matter since it is a densely myelinated structure that was shown at electron microscopy level to make almost no local synapses (Schüz and Munster 1985).

### *2.4 Calculating physical connectivity from the templates*

Calculating the average physical connectivity from the neuronal morphology requires certain assumptions, as well as a definition of what a physical contact is:

1. A physical contact is defined wherever an axon passes closer than some critical distance – $\varepsilon$, to a dendrite. The critical distance is the only free parameter of the model, and its value must be provided according to morphological considerations. These considerations are discussed in Sect. 4.2.
2. The creation of physical contacts is governed solely by the constraints imposed by the geometry of the axonal and dendritic trees. This statement is true when no repulsive or attractive forces are assumed to exist between the axons and dendrites. This assumption is supported by the fact that neuronal morphology is largely conserved across brain regions, and even across species, despite the exposure to different local environments (i.e., different neuronal compositions).
3. The critical distance, $\varepsilon$, must be much smaller than the average segment length of the axons and dendrites. In most cases, $\varepsilon$ is of the order of microns, and the average segment length is of the order of tens of microns, rendering the assumption valid.

Having established the assumptions, the general layout of the formulation is the following. Each volume element in space contains segments of axons and dendrites whose density and directionality are described by the corresponding templates. In accordance with assumption 2, the statistics of the axonal and dendritic segments at that volume element are independent. The formulation uses these statistics to calculate the chance that an axon segment will pass closer than $\varepsilon$ to some dendritic segment. According to assumption 1, this should give an estimate of the number of contacts formed in that voxel.

In a more rigorous way, Fig. 1 shows a general scheme of the problem. A dendritic segment of length $l$ and direction $\Omega_D$ is positioned around $\boldsymbol{r}$. Axonal segments with direction $\Omega_A$ will form contacts according to assumption 1 only if they pass through the rectangular area, standing perpendicular to the plane defined by $\Omega_D$ and $\Omega_A$. Since the templates are a measure of segment flux, the number of axonal segments that pass through the rectangle is

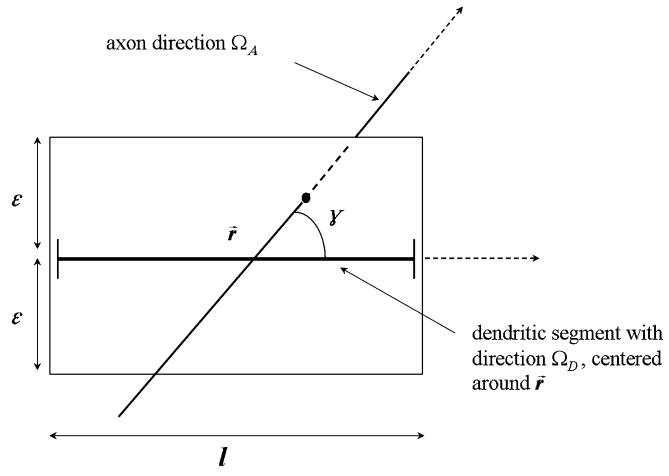


**Fig. 1.** General scheme for evaluating close proximity between axons and a segment of dendrite. See methods for details

$$2\varepsilon l F_A(\boldsymbol{r},\Omega_A)\sin\gamma(\Omega_D,\Omega_A) \tag{2}$$

where $\gamma$ is the angle between the directions $\Omega_D$ and $\Omega_A$, and the term $\sin\gamma(\Omega_D,\Omega_A)$ is the correction due to the oblique angle of the axonal segments passing through the rectangle. Assumption 3 is used here to discard the more complex geometry required around the two ends of the dendritic segment. By taking into account not just one segment but the entire dendritic flux around $\boldsymbol{r}$, the average number of contacts, $\mathrm{d}N(\boldsymbol{r},\Omega_A,\Omega_D)$, created by dendritic and axonal segments with directions $\Omega_D$ and $\Omega_A$, respectively, in a volume element $\mathrm{d}V$ around $\boldsymbol{r}$ is

$$\mathrm{d}N(\boldsymbol{r},\Omega_A,\Omega_D) = 2\varepsilon F_A(\boldsymbol{r},\Omega_A)F_D(\boldsymbol{r},\Omega_D) \times \sin\gamma(\Omega_A,\Omega_D)\mathrm{d}V \tag{3}$$

The total number of contacts expected between the two neurons is the sum of contributions of all the possible directions and voxels. Thus, by integrating Eq. 3

$$N = 2\varepsilon \int_V \int_{\Omega_D} \int_{\Omega_A} F_A(\boldsymbol{r},\Omega_A)F_D(\boldsymbol{r},\Omega_D) \times \sin\gamma(\Omega_A,\Omega_D)\mathrm{d}\Omega_A\mathrm{d}\Omega_D\mathrm{d}V \tag{4}$$

Equation 4 gives the average number of contacts for the case where the cell bodies of the innervating and innervated neurons overlap. It can be slightly modified to a convolution form. $N(\boldsymbol{r}_{\mathrm{ref}})$ is the average number of contacts if the postsynaptic cell body is displaced by $\boldsymbol{r}_{\mathrm{ref}}$ from the presynaptic cell body.

$$N(\boldsymbol{r}_{\mathrm{ref}}) = 2\varepsilon \int_V \int_{\Omega_D} \int_{\Omega_A} F_A(\boldsymbol{r},\Omega_A)F_D(\boldsymbol{r}-\boldsymbol{r}_{\mathrm{ref}},\Omega_D) \times \sin\gamma(\Omega_A,\Omega_D)\mathrm{d}\Omega_A\mathrm{d}\Omega_D\mathrm{d}V \tag{5}$$

For the application of Eq. 5 to real data the integrals are replaced by sums. The indices $i, j$ cover all the principal directions, and $k$ covers all the voxels. $\Delta V(k)$ is the volume of voxel $k$.

$$N(\boldsymbol{r}_{\mathrm{ref}}) = 2\varepsilon \sum_k \sum_i \sum_j F_A\big(\boldsymbol{r}_k,\Omega_j\big)F_D(\boldsymbol{r}_k-\boldsymbol{r}_{\mathrm{ref}},\Omega_i) \times \sin\gamma\big(\Omega_i,\Omega_j\big)\Delta V(k) \tag{6}$$

### *2.5 Calculation of additional properties*

The statistical distribution of the contact number around the mean calculated by Eq. 5 is also of interest. In the model of Liley and Wright (1994), a Poisson distribution was assumed. The assumption of Poisson distribution is based on the argument that the average number of contacts is the sum of many small contributions from all the contact probabilities in the voxels. Such sums usually yield Poisson distributions; however, a crucial condition for Poisson distributions is that all the contributions be independent of each other, and this condition is not always valid for the model. Simulations on artificial trees (data not shown) reveal that the actual distribution is usually broader than Poisson distributions, having larger high value tails. Yet it could be approximated by a Poisson distribution provided that the cell type is relatively uniform. Pyramidal neurons are remarkably uniform (see Sect. 3), so a Poisson distribution is a reasonable approximation for the statistics of their number of physical contacts. Also, Poisson distributions of boutons along axon collaterals have been previously described, supporting a Poisson model for connectivity (Hellwig et al. 1994; Shepherd et al. 2002).

A powerful outcome of the model described is the relative ease with which any property of the physical contacts can be calculated provided that the average intensity of that property is known for any point in space. Such properties could be the average branch order or dendritic width at contact points. As an example, the calculation of the average presynaptic distance (along the axon) between the cell body and the contact point was performed. To this end, a 3D function $G(\boldsymbol{r})$ calculated from the reconstructions of the axons ($n = 11$) describes the average distance of axon collaterals from the soma at position $\boldsymbol{r}$. The average presynaptic distance, $\langle G(r)\rangle$, is then derived from Eq. 5 to be

$$\langle G(r)\rangle = \frac{2\varepsilon}{N(\boldsymbol{r}_{\mathrm{ref}})} \int_V \int_{\Omega_D} \int_{\Omega_A} \times G(\boldsymbol{r})F_A(\boldsymbol{r},\Omega_A)F_D(\boldsymbol{r}-\boldsymbol{r}_{\mathrm{ref}},\Omega_D) \times \sin\gamma(\Omega_A,\Omega_D)\mathrm{d}\Omega_A\mathrm{d}\Omega_D\mathrm{d}V \tag{7}$$

## 3 Results

### *3.1 Templates of layer 5 pyramidal neurons at the rat somatosensory cortex*

The axonal and dendritic morphologies of pyramidal neurons showed a high degree of stereotypy. Typical

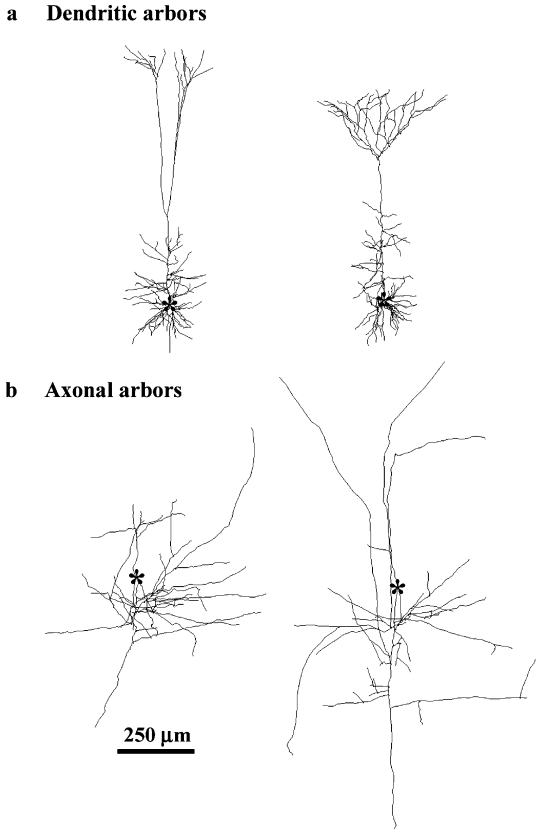


**Fig. 2.** Characteristic dendritic (**a**) and axonal (**b**) trees of two layer 5 pyramidal neurons. Cell body positions are marked by *asterisks*

examples of reconstructed dendritic trees are shown in Fig. 2a. The dendrites of each cell are divided into three parts: (1) basal dendrites, branching out of the cell body in a radial manner; (2) oblique apical dendrites, branching out of the apical dendrite in right angles, up to the border of layers 3/4; (3) apical tuft dendrites, which include the massive branching of the apical dendrite in layers 1 and 2. The combined length of the basal and oblique apical dendrites was measured to be $6.3 \pm 0.98$ (mean $\pm$ SD) mm per cell (CV of 15%). Typical examples of reconstructed axonal trees are shown in Fig. 2b. The axon main trunk projected down from the cell body straight into the white matter. Local connectivity occurred by collaterals that branched out of the main trunk at 5–6 points 100–400 µm below the cell body. Soon after leaving the main trunk, the collaterals branched extensively, sending long projections up to layer 1 and into neighboring columns. The combined length of all collaterals that projected up to 300 µm from the axis defined by the apical dendrite was measured to be$5.9 \pm 1.14$ mm (CV of 19%). The small CV values of the dendritic and axonal lengths reflected the high uniformity between pyramidal neurons. This high degree of stereotypy makes them ideal for averaging into templates.

The templates are by definition multidimensional, so only cross sections through them could be plotted. Cross sections of the dendritic template through the $x, y$-plane for various principal directions are shown in Fig. 3a–c.

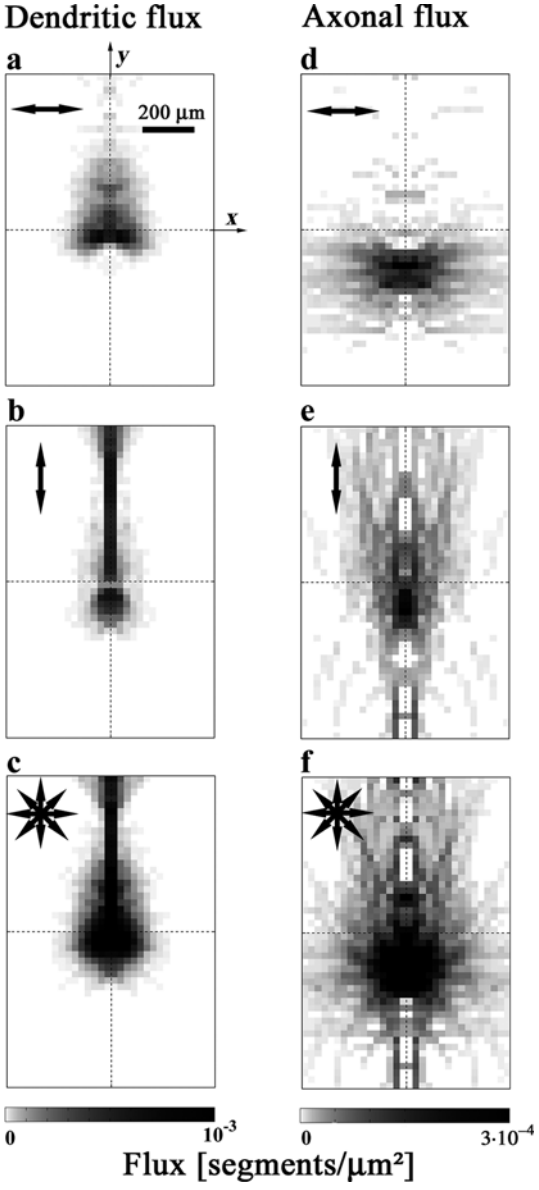


**Fig. 3.** Plots of the dendritic (**a–c**) and axonal (**d–f**) templates at the $x, y$-plane for various principal directions. **a,b** Intensity of the dendritic flux parallel to the $x$-axis and $y$-axis, respectively. **c** Combined intensity of the dendritic flux in all directions. **d,e** Intensity of the axonal flux parallel to the $x$-axis and $y$-axis, respectively. **f** Combined intensity of the axonal flux in all directions. Cell body positions are at the frame centers. *Color bars* of the dendritic and axonal templates are shown at the bottom. Units are those of flux (segments/µm$^2$). Note the different intensity scales for dendrites and axons

Figure 3a shows the template for the principal direction $\{1, 0, 0\}$. High flux was observed around the cell body and in the region of the oblique apical dendrites. Figure 3b shows the template for dendritic segment for the principal direction $\{0, 1, 0\}$. Here, high flux was restricted to a narrow region around the apical dendrite and another region right below the cell body. The integral flux of all the directions is plotted in Fig. 3c. Note the high resemblance to the general span of the dendritic reconstructions in Fig. 2a. Figure 3d–f shows the same data for the axonal template. The axon collaterals

projected parallel to the $x$-axis mainly below the cell body (Fig. 3d), while collaterals parallel to the $y$-axis were found mainly above the cell body (Fig. 3e) due to the projections to layer 1. The above results are in agreement with previous findings also defining average axonal and dendritic fields of various neocortical neurons (Krone et al. 1986). Figure 3a–f is drawn in the same spatial scale to illustrate that the axon was more diffuse compared to the dendrites. The symmetrical appearance of the templates is a direct consequence of implementing the cylindrical symmetry assumption of pyramidal neurons (see methods).

In order to derive the axonal length to a contact, the average length from the cell body along the axons to each voxel was calculated (Fig. 4). Voxels in which no axon was present are uncolored. As expected, the axonal distance increased the further the voxel was from the origin (cell body).

### 3.2 Predicting connectivity

Autapses are synapses formed between axons and dendrites of the same neuron. They could be regarded as physical contacts occurring when the axonal and dendritic templates share the same origin. This is also essentially the case for pre- and postsynaptic neurons where the cell bodies nearly touch. To test the results of the model, we compared the prediction for physical autapses to the real morphological data. Neurons that had both their axons and dendrites reconstructed were chosen ($n = 11$), and a computerized search for all occurrences of a dendrite and an axon passing closer than 4 μm was performed. The value of 4 μm was chosen to be larger than the estimated reconstruction error of 2–3 μm. The average number of such appositions per neuron was found to be $9.3 \pm 1.8$. The number of putative autapses per neuron predicted by Eq. 6 with $r_{\text{ref}} = 0$ and $\varepsilon = 4$ μm for neurons cut 30 μm above the cell body was 8.9. The model prediction was therefore only 5% lower than the observed number, well within the range of the data itself. The predicted distribution of autapses around the cell body was calculated by Eq. 3 and is shown in Fig. 5a. Most autapses were formed with dendrites below the cell body, with highest density of autapses found 75 μm under the cell body and up to 75 μm from the main trunk. The actual spatial distribution of the autapses observed in reconstructions is shown

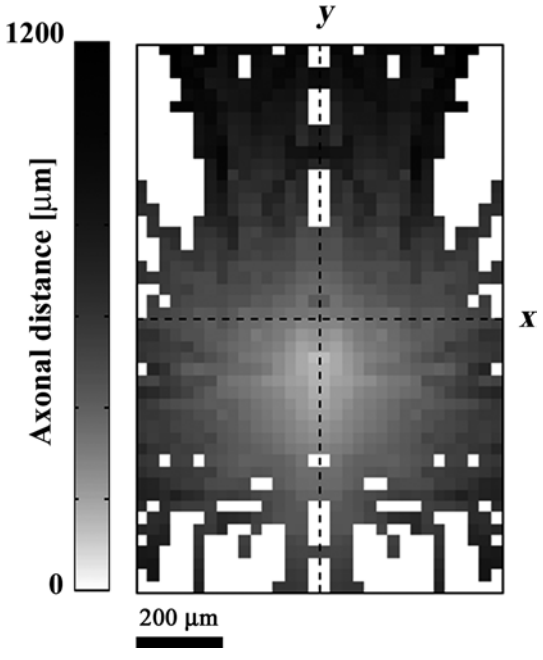


**Fig. 4.** Average axonal distance from the cell body as a function of position, plotted in the $x, y$-plane. The cell body is located at the center of the frame. *White areas* are positions where no axon structure was present in the entire sample

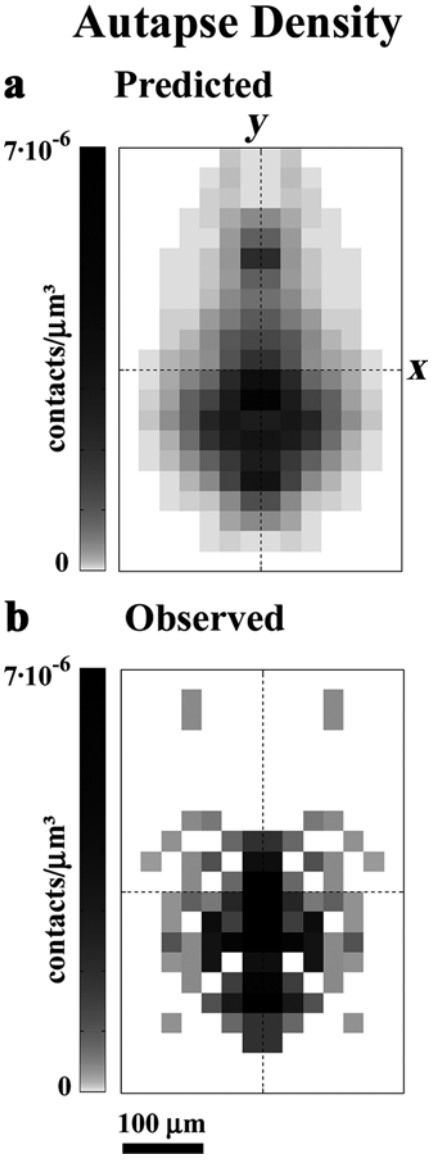


**Fig. 5.** Comparing the predicted (**a**) vs. the observed (**b**) density of morphological autaptic contacts around the cell bodies. The plots are cross sections at the $x, y$-plane of the 3D density distribution. Note the high similarity of the plots both in intensity and spatial form. Units of the *color bars* are contacts/μm$^3$

in Fig. 5b and is similar to the prediction. The average axonal length from the cell body to the apposition point was measured to be 268 μm. Using Eq. 7 and the map in Fig. 4, the predicted axonal length from cell body to contact was calculated to be 292 μm, an error of only 9%.

It is also of interest to compare the model to the results obtained by other anatomical methods. In a detailed light and electron microscopy study, Lübke et al. (1996) estimated the average number of autapses created by layer 5 pyramidal onto itself to be $2.3 \pm 0.9$. This study did not rely on computer reconstructions that have a greater error but searched directly for appositions at the light microscopic level and verified some of these at the EM level. We calculated the $\varepsilon$ value that would give the same prediction of 2.3 autapses, using the linearity of Eq. 6 in $\varepsilon$. The resulting value was $\varepsilon = 0.83$ μm. The average sum of the dendritic and axonal radii of pyramidal neurons is roughly the same, meaning that such an $\varepsilon$ value reflects a very close apposition between the axonal and dendritic membranes. This is consistent with the anatomical definition for synapses used in the described study and with the observation that most autapses were indeed formed on dendritic shafts. The selection of $\varepsilon$ values is further discussed in Sect. 4.2.

The model was then applied to investigate the physical connectivity for neurons in different relative locations. The value for $\varepsilon$ was set to 1 μm, thus ensuring high proximity of the pre- and postsynaptic membranes, according to the average branch radii as discussed above. By changing $r_{\text{ref}}$ in the $x, y$-plane, the expected number of contacts was predicted by Eq. 6 using $\varepsilon = 1$ μm (Fig. 6). The presynaptic cell body was fixed in the frame center, and the mean number of expected contacts was calculated for different postsynaptic cell body locations. The most striking feature of this connectivity mapping was that the peak occurred when the postsynaptic cell body was located 100 μm below the presynaptic one. This peak connectivity predicted an average of 4.8 contacts,

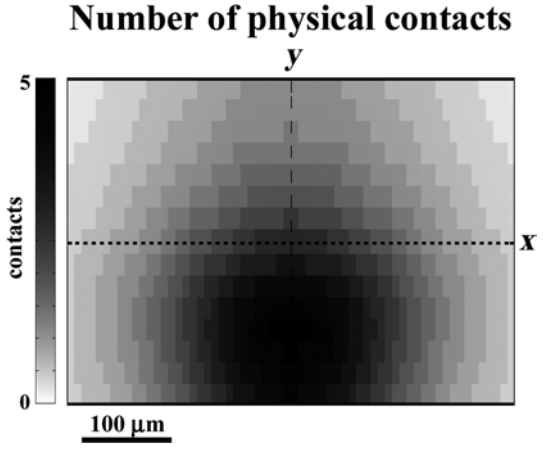


**Fig. 6.** Mean number of appositions of less than 1 μm expected between the axon of a presynaptic cell located at the frame center and the dendrites of the postsynaptic cell whose cell body location is changed in the $x, y$-plane

almost twice the average of 2.8 contacts for two neurons with touching cell bodies.

## 4 Discussion

### *4.1 The model*

This study presents a practical model for deriving the expected number of physical contacts in a pair of neurons from their general morphological statistics and their relative positions. A physical contact is defined as an apposition, closer than a defined distance, between the axons and dendrites of the pre- and postsynaptic neurons, respectively. The motivation for developing such a model is to be able to explore the physical connectivity between neurons, based purely on geometrical factors as the foundation for functional connectivity. The most obvious argument is that physical connectivity sets the high limit for functional connectivity. Moreover, if the functional contacts are taken from a pool of physical contacts in a nonspecific way, a linear relationship is expected between the physical and functional connectivity.

The model itself is based on a limited set of assumptions and requires a rather small number of neurons (10–15) for the extraction of the morphological statistics. The model is verified to be accurate using three separate methods. (1) A rigorous mathematical derivation of the formulation according to the underlying assumptions. (2) The connectivity predictions for autapses are compared with direct measurements of autapses from reconstructed neurons, with all predictions closer than 10% to the measurements. (3) High compatibility of the predictions for autapses with other anatomical studies (Lübke et al. 1996).

Hellwig (2000) showed that physical connectivity could be measured by superimposing two reconstructions together and computing all the proximity points between their structures. Although this superposition method is simpler to implement and understand than the template method used here, the latter has some unique and inherent advantages. (1) The average number of physical contacts is proved to be linear with the critical distance, $\varepsilon$, which defines a contact (Eq. 5). In the superposition method, it is difficult to assess the influence of the critical distance on the number of contacts. (2) Many additional parameters of the physical connectivity can be easily obtained with little extra computation. A few examples of such parameters include the spatial distribution of contacts, the mean axonal length to contacts, and the mean branch order at contacts. Acquiring these additional data using the superposition method is very costly in computation time. (3) The templates represent the generic information of the cell type. If the need arises to find the physical connectivity between layer 5 pyramidal neurons and a new cell type (e.g., an interneuron), all that is zrequired is to create the templates for the new cell type. The templates give the possibility to make "libraries" of different cell morphologies for the purpose of evaluating

physical connections and for constructing microcircuits of neurons.

### *4.2 Physical connectivity in the neocortex*

When selecting the relevant $\varepsilon$ parameter, several considerations must be made regarding the specific type of connections. For example, when investigating synapses that target the dendritic shaft, the reasonable value of $\varepsilon$ would be the sum of the average radii of the axons and dendrites forming the synapse. On the other hand, when the connection is typically formed on fully developed spines, the effective radius of the dendrite is increased, as should be the $\varepsilon$ value. The $\varepsilon$ value should also reflect measurement and reconstruction errors when a computerized search for contacts is performed, since an $\varepsilon$ value smaller than the measurement error is irrelevant.

Lübke et al. (1996) found $2.3 \pm 0.9$ putative autapses per neuron in the same cell type investigated here (layer 5 pyramidal neurons in the somatosensory cortex). Most of the autapses were formed on dendritic shafts and not on spines. To model the described autaptic connectivity, the $\varepsilon$ value should reflect direct physical contact between the axonal and dendritic membranes. The model is therefore applied using an $\varepsilon$ of 1 μm, which is roughly the average sum of the dendritic and axonal radii. The model prediction for such $\varepsilon$ value is 2.8 autapses per neuron. This similarity of numbers suggests that the mechanism behind autaptic formation can be described purely from geometrical factors.

Markram et al. (1997) and Markram et al. (1998) found the average number of putative synapses between adjacent pyramidal neurons in layer 5 to be in the range of 2–8 synapses per connection with an average of 4.6 ($n = 31$ connections, combining both studies). Using the model with an $\varepsilon$ of 1 μm predicts 2–5 physical contacts, depending on the relative separation of the neuronal cell bodies. For adjacent cell bodies the prediction is similar to the case of autapses (2–3 contacts), while for larger vertical separation of the cell bodies the prediction increases to 4–5 contacts (Fig. 6). These values are somewhat lower than the observed ones probably due to an underestimation of $\varepsilon$. Indeed, in these studies most observed synapses are formed on dendritic spines, which increase the effective radius of the dendrites, therefore requiring an $\varepsilon$ larger than 1 μm.

It is also interesting to note that Hellwig (2000), using $\varepsilon \sim 1$ μm, found very similar values (2–3 physical contacts per pair) between adjacent layer 2/3 pyramidal neurons in the rat visual cortex. Other aspects of the physical connectivity, such as its fall-off as a function of distance, were also similar to those found here for the somatosensory cortex. This possible invariance of physical contact number across brain areas and layers might be an inherent characteristic of all pyramidal neurons due to their similar morphologies. However, such a hypothesis needs further substantiation.

Different connectivity patterns are likely to be found for neuron types in which the axonal and dendritic arborizations are significantly different from pyramidal neurons. For example, the axonal tree of various interneuron types is much denser than that of pyramidal neurons, suggesting that a larger number of contacts will be formed on neighboring neurons. Anatomical studies have shown that interneurons typically place three to five times more synapses on pyramidal neurons as pyramidal neurons place on each other (Tamás et al. 1997; Gupta et al. 2000). This outcome could be expected from the model. However, one should be cautious when using the model on interneurons since some of the synaptic types could clearly not be modeled with the method presented here. There are several reasons for this. Synapses on the cell body that are prevalent in interneurons could not be accounted for since only branched structures can be modeled. Also, the model is unsuitable, due to violation of the nonspecificity assumption, for synapses that clearly show a specific mechanism of formation, such as those created by chandelier cells on the initial segment of pyramidal neuron axons. These types of synapses are to be treated with other methods.

In summary, the presented model provides a powerful tool for interpreting anatomical data. Application of the model will allow the extraction of the geometrical influence on synaptic connectivity between different neuronal types in various brain areas. By isolating deviations from the model predictions it may be possible to identify factors underlying functional connectivity.

*Acknowledgements*. This study was supported by the National Alliance for Autism Research, the Minerva Foundation, the US Navy, the Ebner Center for Biomedical Research, and the Edith Blum Foundation.

## References

Anderson JC, Binzegger T, Kahana O, Martin KA, Segev I (1999) Dendritic asymmetry cannot account for directional responses of neurons in visual cortex. Nat Neurosci 2: 820–824

Braitenberg V, Schüz A (1998) Cortex: statistics and geometry of neural connectivity, 2nd edn. Springer, Berlin Heidelberg New York

Gupta A, Wang Y, Markram H (2000) Organizing principles for a diversity of GABAergic interneurons and synapses in the neocortex. Science 287: 273–278

Hellwig B, Schüz A, Aertsen A (1994) Synapses on axon collaterals of pyramidal cells are spaced at random intervals: a Golgi study in the mouse cerebral cortex. Biol Cybern 71: 1–12

Hellwig B (2000) A quantitative analysis of the local connectivity between pyramidal neurons in layers 2/3 of the rat visual cortex. Biol Cybern 82: 111–121

Krone G, Mallot H, Palm G, Schüz A (1986) Spatiotemporal receptive fields: a dynamical model derived from cortical architectonics. Proc R Soc Lond B Biol Sci 226: 421–444

Liley DTJ, Wright JJ (1994) Intracortical Connectivity of pyramidal and stellate cells: estimates of synaptic densities and coupling symmetry. Network Comput Neural Syst 5: 175–189

Lübke J, Markram H, Frotscher M, Sakmann B (1996) Frequency and dendritic distribution of autapses established by layer 5 pyramidal neurons in the developing rat neocortex: comparison with synaptic innervation of adjacent neurons of the same class. J Neurosci 16: 3209–3218

Markram H, Lübke J, Frotscher M, Roth A, Sakmann B (1997) Physiology and anatomy of synaptic connections between thick tufted pyramidal neurones in the developing rat neocortex. J Physiol 500: 409–440

Markram H, Wang Y, Tsodyks M (1998) Differential signaling via the same axon of neocortical pyramidal neurons. Proc Natl Acad Sci USA 95: 5323–5328

Peters A, Jones EG (eds) (1984) Cellular componenets of the cerebral cortex. Plenum, New York

Polleux F, Morrow T, Ghosh A (2000) Semaphorin 3A is a chemoattractant for cortical apical dendrites. Nature 404: 567–573

Schüz A, Munster A (1985) Synaptic density on the axonal tree of a pyramidal cell in the cortex of the mouse. Neuroscience 15: 33–39

Shepherd GM, Raastad M, Andersen P (2002) General and variable features of varicosity spacing along unmyelinated axons in the hippocampus and cerebellum. Proc Natl Acad Sci USA 99: 6340–6345

Tamás G, Buhl EH, Somogyi P (1997) Fast IPSPs elicited via multiple synaptic release sites by different types of GABAergic neurone in the cat visual cortex. J Physiol 500: 715–738

Uttley AM (1956) The probability of neural connexions. Proc R Soc Lond Ser B 144: 229–240

White EL (1989) Cortical circuits: synaptic organization of the cerebral cortex. Birkhäuser, Boston